teraction between the terminal atoms of the I_3^- anions and the iodine atom on the cyclopentadienyl ring of the cation. The anion Br_2I^- is only 7-10% shorter than I_3^-. Because the terminal atoms of Br_2I^- carry more net negative charge than those of I_3^-, the interaction between the terminal atoms of Br_2I^- and the iodine atom on the 1',6'-diiodobiferrocenium cation would be greater than the analogous interaction in the I_3^- salt. Thus, there is a larger in-stack cation-anion interaction in the Br_2I^- salt than in the I_3^- salt. The increased cation-anion interaction in the Br_2I^- salt effectively reduces the frequency for the ring-metal stretching vibration of the cation relative to what is in the I_3^- salt. In other words, the increased anion-cation interaction in the Br_2I^- salt **9** increases the effective mass of the iodocyclopentadienyl ligand compared to what is in the I_3^- salt **3**.

The dependence of the force constant k on the anion explains the dependence of electron localization in mixed-valence cations on anion, because the energy barrier ΔE_C in the cation increases with decreasing k.[32] (It is seen from Table III that in biferrocenium compounds the situation is the reverse, as it should be.) In short, replacing I_3^- by Br_2I^- in 1',6'-diiodobiferrocenium triiodide increases the in-stack cation-anion interaction, E_{II}, and as a consequence the energy difference W (see Figure 9B) both for cations and for anions increases. Compound **9** has to be heated to ~80 K in order to experience cation electron transferring faster than $\sim 10^7$ s^{-1}, whereas compound **3** achieves this at even 4.2 K.

This type of dependence of the energy difference W on the anion-cation interaction E_{II} also explains reasonably the dependence of electron-delocalization temperature on the substituent molecule X. The electron delocalization in **9** (X = I) occurs at lower temperature than in **10** (X = Br), because the intra-stack anion-cation interaction E_{II} is larger for **10** than for **9**. If **8** (X = Cl) has the same crystal structure as **9** and **10**, the electron delocalization in **8** should occur at higher temperature than that in **10** and **9** as it does, because the substituent Cl atom in **8** carries more net negative charge than the substituent Br and I atoms in **10** and **9**, respectively.

Acknowledgment. We are grateful for support from National Institutes of Health Grant HL13652.

Supplementary Material Available: Figure comparing powder XRD patterns for compounds **2** and **8** (1 page). Ordering information is given on any current masthead page.

(32) Wong, K. Y. Schatz, P. N. *Prog. Inorg. Chem.* **1981**, *28*, 369.

Transmembrane Electron Transfer as Catalyzed by Poly(ethylenimine)-Linked Manganese Porphyrins†

Thomas J. Dannhauser,* Mamoru Nango,‡ Naoto Oku, Kazunori Anzai, and Paul A. Loach

Contribution from the Department of Chemistry and the Department of Biochemistry, Molecular Biology, and Cell Biology, Northwestern University, Evanston, Illinois 60201.
Received November 19, 1985

Abstract: Poly(ethylenimine)-linked manganese porphyrins associate with phospholipid bilayers in a manner that allows the porphyrin to penetrate the membrane to a depth limited by the hydrocarbon spacer linking it to the extremely hydrophilic polymer. Control of the length of this spacer group and the sidedness of the incorporation of these complexes in liposome membranes permit systematic variation of the minimum distances separating two such derivatives incorporated from opposite sides of the membrane bilayer. Examination of transmembrane electron transport as catalyzed by these porphyrin complexes reveals that significant rates of electron transfer are observed only when the edge-to-edge distance separating two porphyrins is approximately 4 Å or less. Comparison to theory and relevance to biological electron transfer are discussed.

The study of electron-transfer reactions associated with biological membranes is hindered by our limited knowledge of the relative locations and orientations of the electrochemical prosthetic groups.[1-4] The use of chemical models to provide insight into possible reactions in biological systems has been a valuable tool.[5-9] In an effort to better understand electron transport in bioenergetic membranes, our laboratory and others have reported model systems in which electrons are transported across lipid bilayers. Some of the membrane-soluble electron-transfer catalysts employed in these systems are ferrocene,[10,11] quinones,[10-13] metalloporphyrins,[14,15] chlorophylls,[16] viologens,[17] ruthenium complexes,[18] and isolated cytochromes.[19] The work of Hinkle[10,11] and Hauska[12,13] showed quinones to be capable of transporting both protons and electrons across a membrane, while ferrocene was demonstrated to be an electrogenic catalyst, that is, capable of electron transport only.[10,11] Our laboratory has shown that

†This research was supported by research grants from the National Science Foundation (PCM-7816669) and the U.S. Public Health Service (GM-26098).

‡Current address: Department of Applied Chemistry, University of Osaka Prefecture, Sakai, Osaka 591, Japan.

*Current address: Department of Chemistry, University of Rochester, Rochester, New York 14620.

(1) Boyer, P. D.; Chance, B.; Ernster, L.; Mitchell, P.; Racker, E.; Slater, E. C. *Annu. Rev. Biochem.* **1977**, *46*, 955-1026.
(2) Capaldi, R. A.; Malatesta, F.; Darley-Usmar, V. M. *Biochim. Biophys. Acta* **1983**, *726*, 135-148.
(3) Hauska, G.; Hurt, E.; Gabellini, N.; Lockau, W. *Biochim. Biophys. Acta* **1983**, *726*, 97-133.
(4) Trumpower, B. L. *J. Bioenerg. Biomembr.* **1981**, *13*, 1-24.
(5) Ibers, J. A.; Holm, R. H. *Science (Washington, DC)* **1980**, *209*, 223-235.
(6) Traylor, T. G. *Acc. Chem. Res.* **1981**, *14*, 102-109.
(7) Strothkamp, K. G.; Lippard, S. J. *Acc. Chem. Res.* **1982**, *15*, 318-326.
(8) Kong, K. L. Y.; Spears, K. G.; Loach, P. A. *Photochem. Photobiol.* **1982**, *35*, 545-553.
(9) Fujita, I.; Davis, M. T.; Fajer, J. *J. Am. Chem. Soc.* **1980**, *100*, 6280-6282.
(10) Hinkle, P. *Biochem. Biophys. Res. Commun.* **1970**, *41*, 1375-1381.
(11) Hinkle, P. C. *Fed. Proc., Fed. Am. Soc. Exp. Biol.* **1973**, *32*, 1988-1992.
(12) Futami, A.; Hurt, E.; Hauska, G. *Biochim. Biophys. Acta* **1979**, *547*, 583-596.
(13) Futami, A.; Hauska, G. *Biochim. Biophys. Acta* **1979**, *547*, 597-608.

0002-7863/86/1508-5865$01.50/0

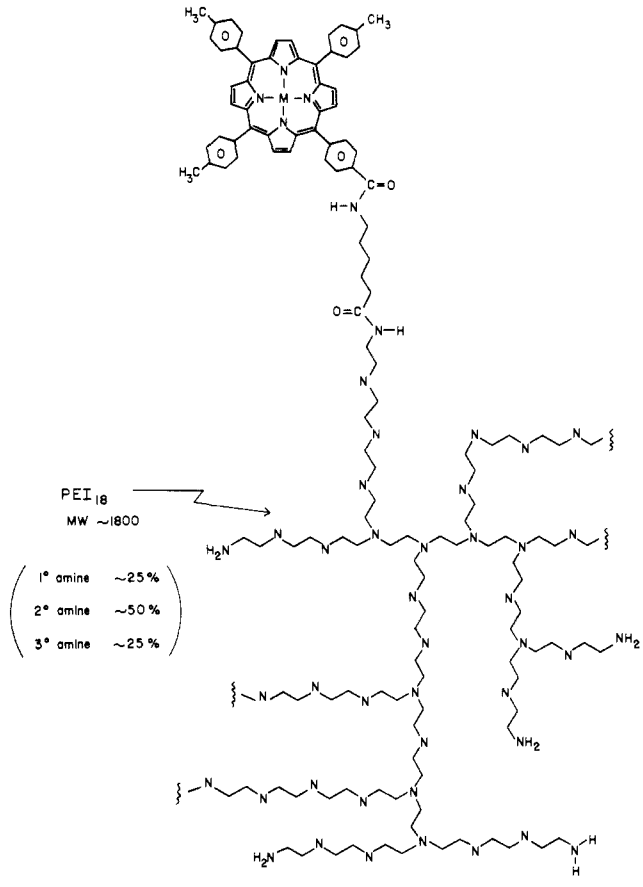

Figure 1. Schematic representation of a PEI-linked porphyrin. The nomenclature PEI-C_n-(M)TPP is used to describe these complexes: PEI is poly(ethylenimine), (M)TPP represents the linked free base or metalloporphyrin, and C_n represents the aliphatic spacer group in which n equals the number of methylene units between the amide bonds.

metalloporphyrins can serve as electroneutral catalysts, transporting both protons and electrons across a lipid bilayer.[14,15]

So far, little information has been obtained from these particular models about the details of electron-transfer reactions, such as the effects of distance and orientation of the redox groups on the rates of electron transport. To our knowledge, the effects of systematically varying the relative orientations of electron donor and acceptor have not been studied experimentally. Experimental evaluation of the effects of distance and differences in electrochemical potential has been examined by studying electron-transfer reactions between a donor and an acceptor in a dilute frozen solution.[20-22] Lee and Hurst used a phospholipid bilayer to separate their donor-acceptor pair.[18] Alternatively, the donor and acceptor have been separated by covalently binding these to a rigid organic spacer.[23,24] Recently, natural proteins have been employed as a pseudo-rigid matrix.[25-27] However, with the exceptions of the hybrid hemoglobins of McGourty et al.[27] and the donor-acceptor complexes containing relatively small, rigid spacer groups,[23,24] the distances separating the electron donor and acceptor molecules are still approximate values.

We have recently reported the synthesis and characterization of water-soluble PEI-linked porphyrins (see Figure 1) and their association with lipid membranes.[28] This model system was developed in order that the distance the porphyrin redox center can penetrate into the bilayer could be restricted and systematically varied, allowing evaluation of the distance dependence of electron transport between isoenergetic redox centers. In this paper, we report the results of ground-state transmembrane electron transfer using PEI-manganoporphyrin complexes.

Experimental Section

Commercially available reagents were used without further purification except as otherwise stated. Polyethylenimine (PEI)-linked porphyrin and metalloporphyrin derivatives were prepared as previously described.[28]

Electron Transfer Assay. Transmembrane electron transport from an external reductant, reduced indigotetrasulfonic acid ($ITSAH_2$), to ferricyanide trapped within an egg phosphatidylcholine (PC) liposome as mediated by a catalyst (e.g., a metalloporphyrin) incorporated in the vesicle bilayer was studied by monitoring the appearance of oxidized indigotetrasulfonic acid (ITSA, λ_{max} ~605 nm). Conditions for this assay were nearly identical with those previously published.[14]

Preparation of Small Unilamellar Vesicles (SUV's) Incorporating PEI-Porphyrin Complexes. Egg phosphatidylcholine (100 mg, Sigma, type III-E) was dissolved in a few milliliters of $CHCl_3$. An aliquot of the desired PEI-linked porphyrin in $CHCl_3/CH_3OH$ (1:1) was added and mixed, and the solvent was removed on a rotary evaporator. The porphyrin-lipid film was suspended in 3.0 mL of 0.1 M $K_3Fe(CN)_6$ in 0.4 M imidazole buffer, pH 7.0, by gentle swirling. The smooth, turbid suspension was sonicated at 0° C under a stream of nitrogen by using a Branson Model 200 Sonifier, output = 3, 50% duty cycle for 10-12 min. The vesicle samples were then applied to a Sephadex G-25-80 gel filtration column (1.5 cm i.d. × 15 cm long) using 0.15 M KCl in 0.4 M imidazole buffer, pH 7.0, as the eluting buffer. The fraction containing the SUV's (diameter approximately 300 Å by electron microscopy (see Figure 2)) was collected with little dilution (about 20%). Oxygen was removed from the vesicles by passing argon gas over and through the vesicle solution for about 1 hour or by submitting the vesicles to 5 or 6 cycles of low vacuum/N_2 (g) purge. The vesicles were then stored under inert gas until needed for the electron transfer assay, which was performed the same day.

Preparation of Large Unilamellar Vesicles (LUV's) Incorporating PEI-Porphyrin Complexes. For the preparation of LUV's, SUV's containing 60 mg of egg phosphatidylcholine, 8 μmol of dicetylphosphate (DCP), and PEI-porphyrin were made in 2 mL of 0.2 M $K_3Fe(CN)_6$ in 0.4 M imidazole buffer, pH 7.0. This SUV suspension was mixed with 90 μmol of octylglucoside and left to stand for a few hours.[26] The turbid suspension was then passed through a gel filtration column (G-25) by using the above ferricyanide-containing buffer as the eluant. Two additional passes through a G-25 column (now eluting with 0.3 M KCl in 0.4 M imidazole buffer, pH 7.0) served to remove the external ferricyanide as well as some residual octylglucoside. The resulting vesicles have an average diameter of about 1000 Å (see Figure 2) and contain some residual detergent, although this was estimated to be less than one molecule per 200 lipids, based on ^{14}C-labeling studies (Figure 3). Oxygen was removed in the same manner as with SUV's, and the LUV's were stored under argon until used in the electron transfer assay later the same day.

Preparation of Vesicles with Externally Incorporated PEI-Porphyrins. Preformed vesicles (SUV's or LUV's) containing internally trapped ferricyanide were mixed with an aqueous solution of a PEI-linked porphyrin. The porphyrin penetrated into the vesicle membrane, but because of the impermeability of the lipid bilayer to the PEI polymer, the porphyrins were incorporated only from the external surface of the vesicles.[28] The vesicles were deoxygenated as described above.

(14) Runquist, J. A.; Loach, P. A. *Biochim. Biophys. Acta* **1981**, *637*, 231-244.
(15) Loach, P. A.; Runquist, J. A.; Kong, K. L. Y.; Dannhauser, T. J.; Spears, K. G. *Electrochemical and Spectrochemical Studies of Biological Redox Components*; Kadish, K., Ed.; Advances in Chemistry 201; American Chemical Society: Washington, DC, 1982; Chapter 22, pp 515-561.
(16) Ford, W. E.; Tollin, G. *Photochem. Photobiol.* **1982**, *35*, 809-19.
(17) Ford, W. E.; Otvos, J. W.; Calvin, M. *Proc. Natl. Acad. Sci. U.S.A.* **1979**, *76*, 3590-93.
(18) Lee, L. Y. C.; Hurst, J. K. *J. Am. Chem. Soc.* **1984**, *106*, 7411-7418.
(19) Tabushi, I.; Nishiya, T.; Shimomura, M.; Kunitake, T.; Inokuchi, H.; Yagi, T. *J. Am. Chem. Soc.* **1984**, *106*, 219-226.
(20) Miller, J. R.; Hartman, K. W.; Alrash, S. *J. Am. Chem. Soc.* **1982**, *104*, 4296-4298.
(21) Guare, T.; McGuire, M.; Strauch, S.; McLendon, G. *J. Am. Chem. Soc.* **1983**, *105*, 616-618.
(22) Beitz, J. V.; Miller, J. R. *J. Chem. Phys.* **1979**, *71*, 4579.
(23) Calcaterra, L. J.; Closs, G. L.; Miller, J. R. *J. Am. Chem. Soc.* **1983**, *105*, 670-671.
(24) Miller, J. R.; Beitz, J. V.; Huddleston, R. K. *J. Am. Chem. Soc.* **1984**, *106*, 5057-5068.
(25) Winkle, J. R.; Nocera, D. G.; Yocum, K. M.; Bordignon, E.; Gray, H. B. *J. Am. Chem. Soc.* **1982**, *104*, 5798-5800.
(26) Isied, S. S.; Worvsila, G.; Atherton, S. J. *J. Am. Chem. Soc.* **1982**, *104*, 7659-7661.
(27) McGourty, J. L.; Blough, N. V.; Hoffman, B. M. *J. Am. Chem. Soc.* **1983**, *105*, 4470-4472.
(28) Nango, M.; Dannhauser, T.; Huang, D.; Spears, K.; Morrison, L.; Loach P. *Macromolecules* **1984**, *17*, 1898-1902.

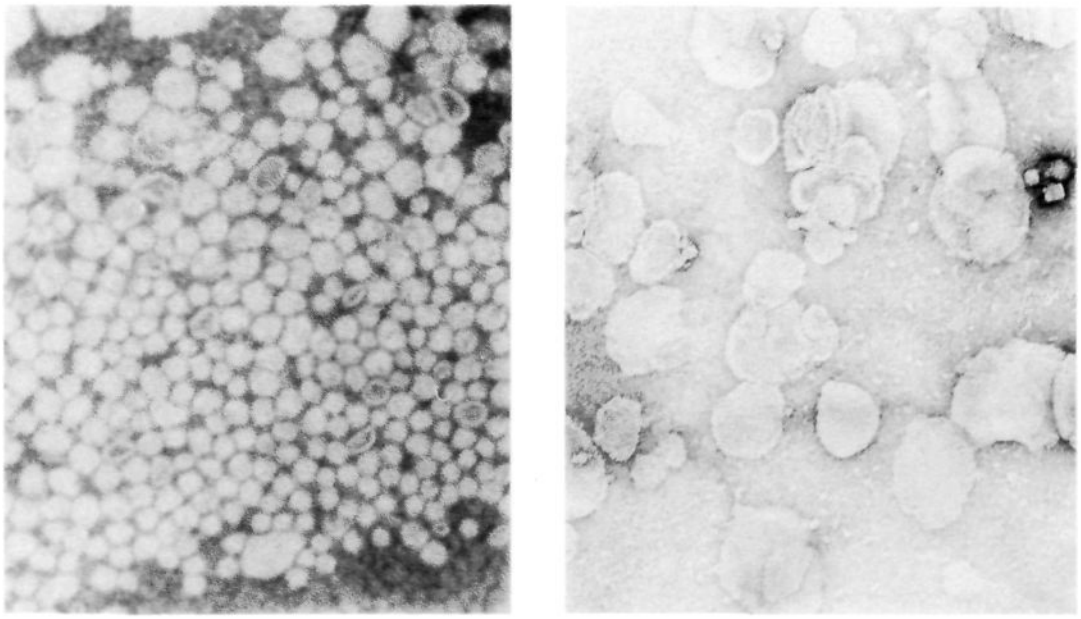

Figure 2. Electron micrographs of SUV (left) and LUV (right) preparations. SUV's were stained with 1% phosphotungstic acid; LUV's were stained with 2% uranyl acetate. The bar below each micrograph corresponds to 1000 Å.

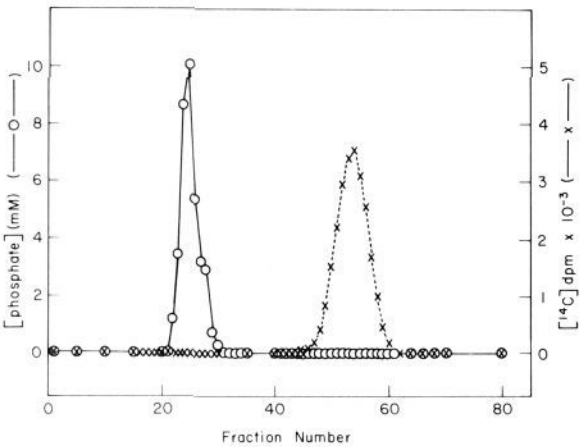

Figure 3. Separation of LUV's and octylglucoside by gel filtration chromatography. LUV's were prepared by using (1-^{14}C)*N*-octyl-β-D-glucoside (Research Products International Corp.). 1.0 mL of sample was applied to a Sephadex G-25-80 column (1.5 cm i.d. × 42 cm long) and eluted with 0.4 M imidazole buffer, pH 7.0, containing 0.1 M K_3-$Fe(CN)_6$. 50 drops (about 1.15 mL) were collected for each fraction. 2 μL of each fraction were used to count the radioactivity of ^{14}C (X) and 10 μL were used for phosphate assay (O).

Results and Discussion

Effects of Varying the Spacer Length (C_n) in PEI–C_n–MnTTP. The PEI polymer-linked porphyrins used in this work have three important structural features: the PEI polymer, the metalloporphyrin, and the spacer group. The PEI polymer used is relatively small (MW ~ 1800) and highly branched. At pH 7.0, it is highly charged and very water-soluble. In contrast, the manganese porphyrin is an extremely hydrophobic tetratolyl porphyrin derivative. This porphyrin can be directly attached to the PEI polymer, or an intervening linear chain of selected length can be employed to separate the porphyrin from the polymer. We have previously provided evidence[28] that these PEI–porphyrin complexes interact with lipid membranes in the manner diagrammed in Figure 4 (top): the hydrophobic porphyrin and spacer group penetrate into the bilayer but are prevented from diffusing across the bilayer by the membrane-impermeable PEI polymer, which remains in the aqueous phase. By varying the length of the spacer group, the position of the membrane-bound PEI–porphyrin in the bilayer can be systematically changed, and, consequently, the minimum distance separating two such deriv-

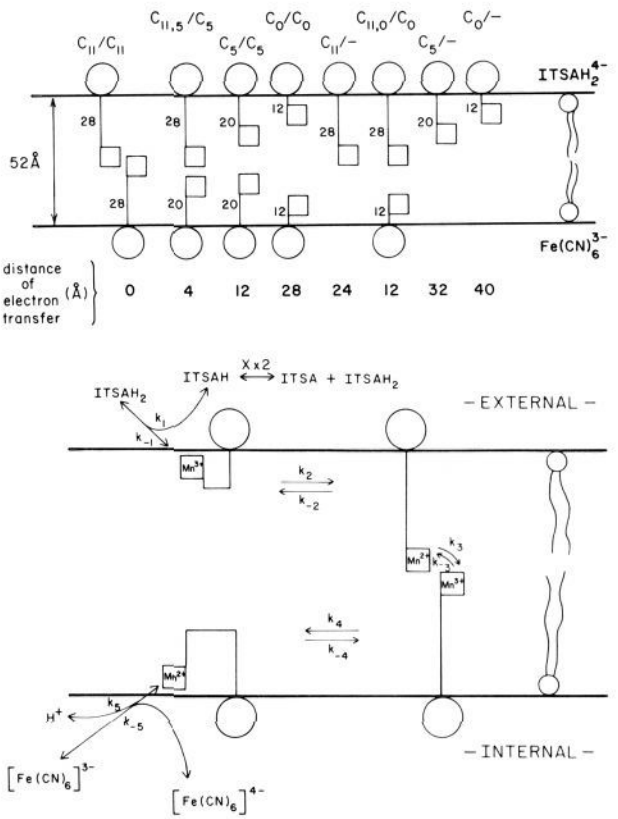

Figure 4. (top) Schematic diagram of minimum distances separating PEI–C_n–MnTTP derivatives inserted from opposite sides of a lipid bilayer. Each polymer porphyrin is represented in its extended conformation. The distance from the PEI/spacer amide carbonyl to the far edge of the porphyrin pyrrole ring is estimated to be the maximum depth the porphyrin can penetrate in the bilayer. See text for further discussion. The notation $C_{11,5}/C_5$ indicates both C_5 and C_{11} PEI–MnTTP derivatives present on the external surface with a C_5 derivative located on the inner membrane surface. (bottom) Proposed scheme for electron transport as catalyzed by PEI–C_{11}–MnTTP. See text for explanation.

Table I. Transmembrane Electron Transfer as Catalyzed by PEI-C_n-MnTTP Derivatives

		SUV		LUV	
catalyst	distance[a] (Å)	k^b (s^{-1} μmol^{-1})	k'^c	k^b (s^{-1} μmol^{-1})	k'^c
C_{11}/C_{11}	0	4.26 ± 0.52[d] (5)[e]	5.96	3.27 ± 0.70 (8)	5.89
$C_{11,5}/C_5$	4	1.51 ± 0.20 (2)	1.51	0.95 ± 0.08 (2)	0.95
C_5/C_5	12	0.35 ± 0.14 (6)	0.49	0.07 ± 0.28 (2)	0.13
$C_{11}/$	24	0.71 ± 0.09 (5)	0.71	0.06 ± 0.28 (6)	0.06
$C_{11,o}/C_o$	12			0.41 ± 0.26 (2)	0.41
C_o/C_o	28	−0.21 (1)	−0.29	0	0
$C_5/$	32	0.03 ± 0.06 (2)	+0.03		
$C_o/$	40	0.18 ± 0.11 (2)	+0.18		

[a] As calculated from Figure 4. [b] Leak rate of 0.21 s^{-1} μmol^{-1} (SUV) or 1.53 s^{-1} μmol^{-1} (LUV's) was subtracted from original result. [c] Calculated on basis of external PEI-C_n-MnTTP only, based on 69% total incorporated on external surface of SUV's and 56% total incorporated on external surface of LUV's. [d] Standard deviation. [e] Number of experimental determinations.

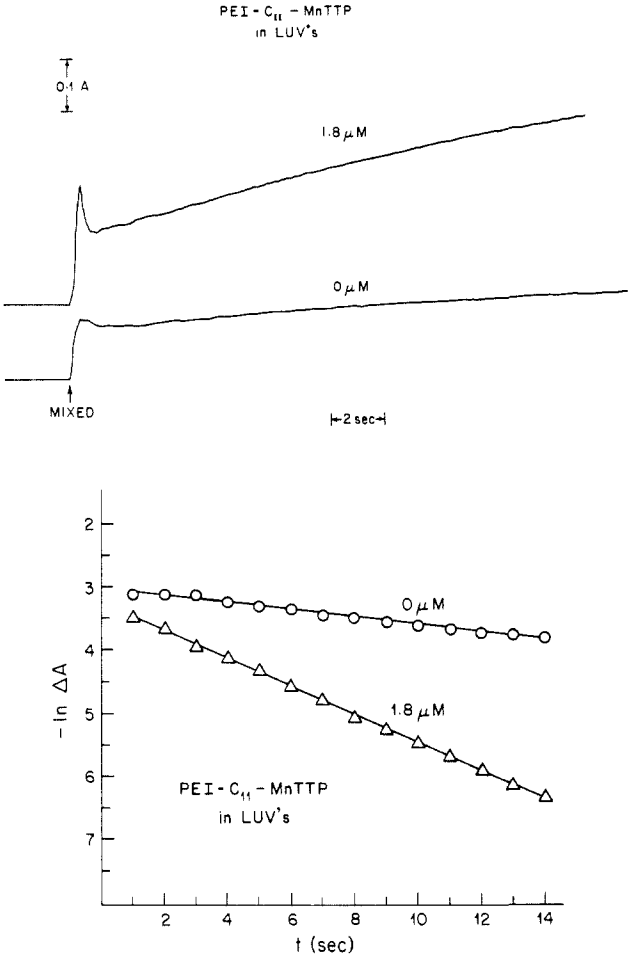

Figure 5. Catalysis of electron transfer across LUV liposomes by PEI-C_{11}-MnTTP incorporated on both sides of liposome bilayer. (top) Time course of absorbance change at 605 nm. The initial absorbance at time of mixing was 0.090. For other details of the assay, see Experimental Section. (bottom) Semilog plot of data in top figure.

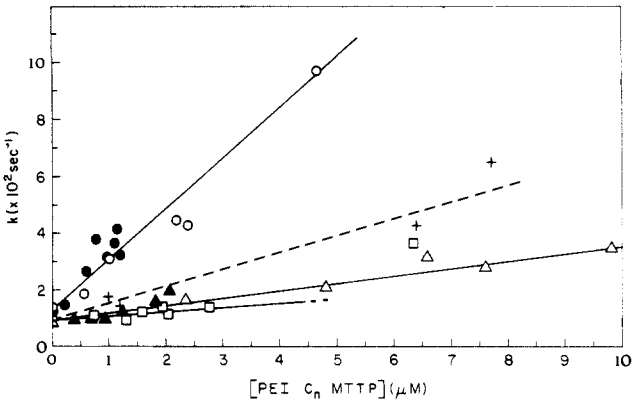

Figure 6. Pseudo-first-order rate constants of transmembrane electron transport vs. external concentration of PEI-C_n-MnTTP catalyst. Concentration of catalyst on external surface calculated as in Table II. PEI-C_{11}-MnTTP present on both sides of LUV (○) and SUV (●) membrane; PEI-C_{11}-MnTTP present only on external surface of LUV's (△) and SUV's (▲); PEI-C_5-MnTTP present on both surfaces of SUV membranes (□); same as last, but with PEI-C_{11}-MnTTP also present on external surface of SUV's, plotted as function of PEI-C_{11}-MnTTP concentration (+).

atives inserted from opposite sides of the membrane can also be varied.

The PEI-porphyrins tested were manganese-substituted C_{11}, C_5, and C_0 derivatives (see Figure 1 for explanation of nomenclature). An example of experimental results obtained and a log plot of the data are shown in Figure 5. The results obtained for each derivative at a variety of concentrations are summarized in Figure 6 and Table I. Unlike monomeric MnTPP,[15] little or no electron transport was catalyzed by PEI-C_5-MnTTP or PEI-C_0-MnTTP, regardless of whether these complexes were present on both sides or only the external surface of the membrane. PEI-C_{11}-MnTTP, when added only to the outside of preformed vesicles, showed low rates of electron transport. However, when this complex was present on both sides of the vesicle membrane, the rate of transmembrane electron transport catalyzed by PEI-C_{11}-MnTTP was increased substantially and was approximately $^1/_4$ that of MnTPP.

Control experiments were conducted employing PEI-C_{11}-H_2TTP or PEI-C_{11}-ZnTPP present on both sides of the vesicle bilayer. Our earlier results with free porphyrins had shown that the redox potentials of the free base and zinc porphyrins lie outside the range required for electron transport catalysis in this model system.[14,15] Thus, this control should allow us to observe any structural effect of the PEI polymer-linked porphyrins on transmembrane electron transport. The rate observed was unchanged from the background, showing that the PEI polymer-linked free base porphyrin was not catalytic and did not create any substantial membrane defects causing leakage.

The significant rates of electron transport catalyzed by PEI-C_{11}-MnTTP were of special interest. To further explore distance effects with these surface anchored catalysts, we prepared mixed systems containing the C_5 derivative on both sides of the membrane and then added the PEI-C_{11}-MnTTP so that it was available only from the external surface. Since little catalysis was observed for symmetrically prepared PEI-C_5-MnTTP, the enhanced catalysis observed in the mixed system was assumed to involve electron transfer from the external PEI-C_{11}-MnTTP to a PEI-C_5-MnTTP located on the inside half of the vesicle bilayer (see Figure 6 and Table I).

Effects of Size in Liposome Preparations. Two types of liposome preparations (SUV's and LUV's) were used for the electron-transfer assay. The properties of these different vesicles are summarized in Table II. The SUV values are consistent with those reported by others.[29,30] In addition, the amount of ferri-

(29) Mimms, L. T.; Zampighi, G.; Nozaki, Y.; Tanford, C.; Reynolds, J. A. *Biochemistry* **1981**, *20*, 833-840.

Table II. Properties of SUV's vs. LUV's

	diam (Å)	trapped vol (μL/μmol PC)	lipids per vesicle	% incorprtn of catalyst	catalysts per vesicle[a]
SUV's	300	0.5	6 000	80	2
LUV's	800	2.3	50 000	40	20

[a] Average number of catalysts calculated per vesicle when the porphyrin concentration was determined to be 1×10^{-6} M in the electron transfer assay (0.25 mL vesicle sample +2.5 mL reductant). This assumes all the porphyrin molecules are in the lipid of the liposomes.

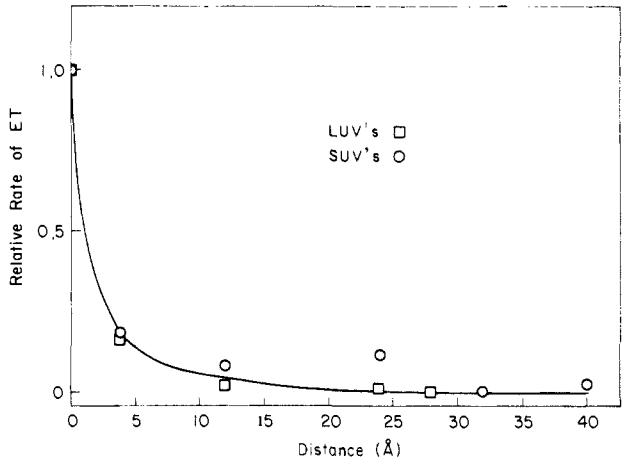

Figure 7. Relative electron transport as a function of the distance separating two PEI-linked porphyrins inserted from opposite sides of the bilayer. The distances are calculated by using the data from Figure 4. The notation is the same as used in Figure 4.

cyanide observed to be trapped within our SUV and LUV preparations is in good agreement with these calculations. Our SUV preparations have the advantage of size homogeneity, relatively good stability, and easy preparation. We were concerned however that the PEI–porphyrin incorporation per vesicle was not statistically homogeneous because of the small size of the SUV's. The octylglucoside method of LUV preparation allowed us to compensate for the shortcomings of the SUV preparation. Although these are perhaps not properly described as LUV's according to characteristics given by Szoka and Papahadjopoulos,[31] their size and internal volumes are significantly larger than SUV's. In addition, the LUV bilayer more closely approximates the planar character of most biological membranes; the inner and outer halves of SUV bilayers are very asymmetric because of their small radius of curvature. However, the LUV's are more difficult to prepare and sometimes have significantly higher leak rates than SUV's.

Despite the significant differences of these two liposomal preparations, the results obtained with both systems are very similar (see Figures 6 and 7). This internal consistency is indicative that the interaction of the PEI–porphyrins with lipid membranes is similar for both SUV's and LUV's and suggests there was a symmetrical distribution (in terms of PEI–C_n–MnTTP/P-Lipid) of the PEI-linked catalyst on the two halves of the bilayer. The data further indicate that lipid packing in different membrane structures has little effect on the electron transfer observed in these models. Most important, it demonstrates that the different electron-transfer rates obtained with different combinations of PEI–porphyrins are in fact due to the inherent properties of these PEI–porphyrin complexes, not because of chance interactions of these derivatives with a specific membrane preparation.

Analysis and Comparison with Theory. Independent evaluation of the distance between porphyrin centers introduced on opposite sides of the lipid bilayer is difficult to obtain. We felt fluorescence quenching or excited singlet state energy transfer between appropriate porphyrins[32] were not useful methods because the lateral motion of a porphyrin in its excited singlet state would be slow relative to decay of this state. Thus, a porphyrin molecule in one half of the bilayer would seldom experience an excited porphyrin in the opposite half. A more promising measurement would involve the transfer of excited triplet state energy, but the distances that could be accurately measured are much more restricted. Because of these limitations we have not yet attempted such measurements.

To allow a more detailed evaluation of our results, we have constructed molecular models of the PEI–porphyrins and from these estimated the position of the porphyrins in the bilayer. The thickness of egg phosphatidylcholine bilayers has been measured by using X-ray diffraction[33] and found to be 52 Å at room temperature or 26 Å per PC molecule. A molecular model of 1-palmitoyl-2-oleoylphosphatidylcholine (16:0/18:1 PC, typical for egg yolk PC[34]) was measured in its extended conformation, and a length of 29 Å calculated. Assuming some shortening of the acyl chains due to random kinks in the acyl chains, the model's dimensions agree well with experimental measurements.

At pH 7.0, the PEI polymer is a very hydrophilic polycation with high and relatively uniform charge density. Considering this and the large amount of water of hydration that is present, it seems unlikely that the PEI polymer could penetrate into the membrane, even the relatively polar but well-packed headgroup region. Therefore, we have assumed the PEI-linked porphyrin penetrates into the membrane up to the PEI/spacer amide carbonyl which is estimated to be at the level of the choline headgroup of the lipid. Figure 4 (top) shows these penetration distances as measured from the PEI–spacer amide carbonyl to the edge of the far pyrrole ring of the porphyrin for each of the PEI-linked porphyrin complexes in their fully extended conformations.

Some refinement of this model is possible. Model studies have shown that the change in free energy for the transfer of a long chain alkane from water to a hydrocarbon solvent decreases linearly as the number of methylene units increase.[35] Assuming a constant driving force to hydrate the charged, hydrophilic PEI polymer, increasing the length of the spacer will change the balance of the opposing energetics of solubilizing the porphyrin and spacer group in the bilayer and polymer in the aqueous phase. A possible result of this would be to increase somewhat the depth that the PEI portion of the PEI-linked porphyrin can penetrate the bilayer as longer spacer groups are attached.

In Figure 4 (top) the estimated distances into the bilayer penetrated by the PEI–porphyrin complexes are estimated by using the extended conformations rather than the statistical average positions, which are expected to be somewhat shorter due to random kinks. However, the system is dynamic, and we presume the conformational changes required to allow these extreme positions to be reached are very rapid.[36]

The magnitude of the above refinements are small and, in fact, tend to cancel one another. We therefore believe the numbers used in Figure 4 (top) are within a few angstroms of the actual values. The minimum distance separating two PEI-linked porphyrins inserted from opposite sides of the membrane can be calculated by subtracting the distance these PEI-porphyrins

(30) Huang, C. *Biochemistry* **1969**, *8*, 344–352.
(31) Szoka, F., Jr.; Papahadjopoulos, D. *Annu. Rev. Biophys. Bioenerg.* **1980**, *9*, 467–508.
(32) Anton, J. A.; Loach, P. A.; Govindjee, *Photochem. Photobiol.* **1978**, *28*, 235–242.
(33) Levine, Y. K.; Wilkins, N. K. F. *Nature (London), New Biol.* **1971**, *230*, 69–72.
(34) Gomperts, B. D. *The Plasma Membrane: Models for Structure and Function*; Academic Press: 1977; p 4.
(35) Tanford, C. *The Hydrophobic Effect: Formation of Micelles and Biological Membranes*, 2nd ed.; Wiley: 1980; pp 7–9.
(36) Chapman, D. *Membrane Fluidity: The Concept and Its Development*, In *Membrane Fluidity in Biology*; Aloia, R. C., Ed.; Academic Press: New York, 1983; Chapter 2, pp 5–42.

penetrate into the bilayer from the width of the lipid membrane (52 Å). Figure 7 shows that the rate of transmembrane electron transfer rapidly decreases with increasing separation. A significant electron transfer occurs only at separation distances of less than 4 Å.

Mechanism of Electron Transfer. The mechanism of electron transfer is presumed to follow a pathway as illustrated in Figure 4 (bottom). Electron transfer occurs from external reduced indigotetrasulfonic acid to an oxidized manganese porphyrin which momentarily assumed a folded position relative to its attached PEI group. The semiquinone form of indigotetrasulfonic acid would be expected to disproportionate rapidly in water. The reduced manganese porphyrin is then viewed as changing to an extended configuration relative to the PEI group. Precedence for transverse bilayer movement of apolar molecules of this size in liposomes in the liquid crystalline state is found in studies of ionophores, such as valinomycin, which function as ion carriers.[37] Electron transfer from this manganous porphyrin to a manganic porphyrin tethered to a PEI molecule on the opposite side of the bilayer can then occur if, in their lateral diffusion, they approach each other sufficiently closely. The electron transfer to ferricyanide is then completed by movement of the manganous porphyrin on the inner half of the bilayer to a folded position near the aqueous interface where it can donate an electron to a ferricyanide molecule. In analogy to our previous studies with iron tetraphenyl porphyrin and iron protoporphyrin IX dimethylester where the rate-limiting step was the reaction with $ITSAH_2$,[14,15] it is assumed that diffusion in a transverse direction (perpendicular to the membrane plane) is fast relative to electron-transfer reactions. Furthermore, at the concentrations employed, electron transfer at the ferricyanide interface is assumed to be faster than that at the $ITSAH_2$ interface. According to the data of Figure 5, the rate-limiting step for the PEI–C_{11}/C_{11} system was predominantly k_1. As the number of carbons connecting the MnTTP to PEI was shortened, the rate-limiting step is assumed to shift to k_3 and thus reflect the increasing distance between MnTTP molecules anchored to their PEI constituents at opposite aqueous interfaces. Because the electron-transfer rates are only slightly above background rates in this latter case, the limited accuracy of the data restricts extensive kinetic analysis.

The apparent exceptions to this overall consistent picture are the results found with externally-added PEI–C_{11}–MnTTP. This system appears to catalyze electron transport at low rates despite the porphyrin being at a distance of about 24 Å from an electron acceptor (ferricyanide) at the internal membrane/water interface. However, in this system ferricyanide is the electron acceptor rather than another manganese porphyrin. The $\Delta E^{\circ\prime}$ between the PEI–MnTTP and ferricyanide is +350 mV relative to an equipotential PEI–MnTTP pair. A 10^9 increase in the tunneling rate is possible for an increased difference of electrochemical potential of 1.0 V,[22,38] assuming all other parameters are constant. In addition, manganese porphyrins exhibit a redox-coupled change in coordination number in the presence of strong ligands,[39,40] while ferricyanide remains hexacoordinate upon reduction. We therefore expect the reorganization energy associated with electron transfer to be substantially decreased when ferricyanide is substituted for PEI–MnTTP as the immediate electron acceptor, thus further increasing the probability of electron transfer.

This same argument also can be used to explain the much smaller distances over which electron transfer occurs in our model system as compared to those of other studies of electron-transfer reactions.[19–22] In contrast to our model, the electron transfer was substantially exergonic in these other systems, thus greatly increasing the probability of electron tunneling at long distances. However, we believe each model system can contribute important information about electron transport, the sum of which is required to ultimately understand the in vivo systems.

In one report of long range electron transport between isopotential redox centers, Lee and Hurst[18] have described a system in which ruthenium complexes were located at opposite sides of a lipid bilayer. The long range isoenergetic electron transfer observed in their studies was very slow ($\tau \sim 20$ min), about two orders of magnitude slower than the rates observed in our model. Such slow processes would be lost in the background leak rates of our model systems. We believe small quantities of natural electron carriers, such as ubiquinone present in the egg yolk PC, may explain the background leak rate we experience. The physical nature of Lee and Hurst's proposed intermediary redox sites used to explain the slow rates of electron transport is unclear to us.

An additional feature of electron transfer in our model is the simultaneous transmembrane proton transport; electron transfer is electroneutral as established by assays in the presence and absence of valinomycin/K^+ or FCCP. Our earlier studies demonstrated that only transmembrane hydroxide or proton transfer could explain the electroneutral electron transport catalyzed by monomeric metalloporphyrins.[14] A redox-linked deprotonation of the metalloporphyrin axial ligand was proposed to explain this coupled electron and proton transfer.[14,15] It is possible that a similar mechanism is operating in electron transfer as catalyzed by PEI-linked porphyrins; that is, both electrons and protons are transferred by manganese porphyrins. However, the effects and possible limitations proton transport may have on the mechanism of electron transfer are unknown. The ability to systematically study this aspect is a unique advantage of our model system.[14,15] By selection and adjustment of concentrations of aqueous redox components and by appropriate choices of PEI-linked catalysts, we feel we can study a specific electrochemical reaction either at the membrane surface or within the highly apolar interior.

Since significant electron transport is observed in our model system only when short distances separate two PEI–porphyrins, it is tempting to suggest that electron tunneling is unimportant in our system. However, at present we only are capable of measuring rates of electron transfer over a relatively limited time range: the leak rate across the vesicle membrane creates a background from which it is difficult to extract additional slow electron-transfer rates, and the mechanics of our assay experiment prevent the examination of very fast electron transfer. We have not yet examined the temperature dependence of electron transfer, although at the high temperature limit both classical outer-sphere and quantum mechanical tunneling treatments of electron transfer can give the same results.[41] Therefore, although our results suggest an outer-sphere mechanism to predominate, we cannot rule out the effects of electron tunneling.

Biological Relevance. It seems certain that for effective coupling of energy-releasing electron-transfer reactions to energy utilization reactions in bioenergetic membranes that electron flow must be efficiently directed from one redox center to another.[42–45] Should these vectorial redox reactions be short-circuited by competing long range electron-transfer reactions, there would either be a major loss in efficiency or coupling might not occur at all. Implicit to the occurrence of long range electron transfer is the existence of a large difference in redox potential and an optimal orientation between donor and acceptor. If biological electron transfer were to occur routinely between redox centers with large differences in electrochemical potential, there would have to be an even larger physical separation between competing reactants to minimize side reactions. Besides the additional longer range organization required by such a system, the substantially fewer redox reactions would severely reduce the opportunity for coupling to energy utilization reactions. Therefore, it is not surprising that there are only a few examples of biological electron transfer between redox centers with large differences in electrochemical potential. Most

(37) Dobler, M. *Ionophores and Their Structures*; Wiley: 1981.
(38) Hopfield, J. J. *Proc. Natl. Acad. Sci.* U.S.A. **1974**, *71*, 3640–44.
(39) Scheidt, W. R. In *The Porphyrins*; Dolphin, D., Ed.; 1978; Vol. III, Chapter 10, pp 463–511.
(40) Hoard, J. L. In *Porphyrins and Metalloporphyrins*; Smith, K. M., Ed.; 1975; Chapter 8, pp 317–380.
(41) Devault, D. *Quart. Rev. Biophys.* **1980**, *13*, 387.
(42) Wikstrom, M.; Krab, K. *Curr. Top. Bioenerg.* **1980**, *10*, 51–101.
(43) Wikstrom, M.; Krab, K.; Saraste, M. *Annu. Rev. Biochem.* **1981**, *50*, 623–655.
(44) Malmstrom, O. G. *Biochim. Biophys. Acta* **1979**, *549*, 281–303.
(45) Mitchell, P. *J. Theor. Biol.* **1976**, *62*, 327–367.

in vivo electron transfer occurs between redox centers with small differences in redox potential, many of which are associated with membranes. Examples include NADH dehydrogenase, bc_1 complexes of mitochondria and photosynthetic bacteria, and the first reactions of mitochondrial cytochrome *c* oxidase.[2,3,42-45] Only the final reaction with molecular oxygen is decidely irreversible.

In this context then, we believe the electron transfer between the isopotential Mn porphyrin centers in our model systems to be highly relevant to in vivo systems. The background leak rates observed in our electron transfer assay are short circuits, possibly due to electron tunneling reactions as well as the effects of possible redox-active impurities in the lipid; the biological membranes also have many possible short circuiting reactions since they contain large amounts of unbound quinones and many other redox centers. In our models, we do not observe significant electron transfer above the background leak rate unless the incorporated PEI-porphyrins are capable of approaching one another to within 4 Å or less. These results suggest that distances separating biological redox components with small differences in electrochemical potential must be similarly small if rapid rates of directed electron transfer are to occur. A future extension of our model will involve synthesis of redox centers having small differences in midpoint potential (e.g., up to about 150 mV) for metalloporphyrins anchored on opposite sides of the bilayer.

Registry No. DCP, 2197-63-9; H^+, 12408-02-5.

Solid-State Structural Characterization of 1,3-Cyclohexanedione and of a 6:1 Cyclohexanedione:Benzene Cyclamer, a Novel Host-Guest Species

Margaret C. Etter,[†] Z. Urbańczyk-Lipkowska,*[†] Donald A. Jahn,[†] and James S. Frye[‡]

Contribution from the Department of Chemistry, University of Minnesota, Minneapolis, Minnesota 55455, and Colorado State University, NMR Center, Colorado State University, Fort Collins, Colorado 80523. *Received December 17, 1985*

Abstract: 1,3-Cyclohexanedione (CHD) forms two stereoisomeric hydrogen-bonded supermolecules in the solid state. Both structures contain chains of enolized CHD molecules with very short hydrogen bonds (O···O < 2.58 Å) between the enolic OH and the carbonyl oxygen of a neighboring molecule. In the nonsolvated crystal form, I, CHD chains form with anti-anti hydrogen-bond stereochemistry. In crystals of II, composed of one guest molecule for every six CHD molecules, hexameric hydrogen-bonded rings of CHD with syn-anti hydrogen-bond stereochemistry form cyclic hosts, called cyclamers, which include a single ordered molecule of benzene. Monodeuteriobenzene and perdeuteriobenzene can also be included in CHD cyclamers. Structure II represents a new class of neutral guest complexes in which the host is a hydrogen-bonded analogue of a macrocyclic crown ether. CHD molecules behave functionally like macrocycles in their ability to trap small molecules in a highly selective manner. The X-ray crystal structures and solid-state ^{13}C CP/MAS NMR spectra of I and II are presented, and the criteria for designing other cyclamer structures with neutral guest molecules is discussed. Crystal data: I, a = 8.193 (5) Å, b = 11.712 (3) Å, c = 6.128 (3) Å, β = 99.44 (4)°, $P2_1/a$, Z = 4, 997 observed reflections; II, $a = b$ = 18.127 (7) Å, c = 10.542 (3) Å, $\alpha = \beta$ = 90°, γ = 120°, $R\bar{3}$, Z = 18, 764 observed reflections.

The importance of cryptands, cavitands, and chorands (crown ethers) as models for enzyme-substrate interactions has been the subject of intensive research during the last decade. Chemically diverse hosts have been designed, and a wide range of cavity sizes and types have been engineered.[1] The chemical and structural properties of the supermolecular host-guest species have been studied in detail, and these compounds have found many important applications based on their ability to selectively bind cations[2] and to serve as chiral recognition hosts for the separation of enantiomeric materials.[3] More recently efforts have been devoted to designing hosts that bind neutral small molecules.[4] All synthetic efforts in these areas have involved the design of σ-bonded macromolecules as the host species.

In this paper we describe a new approach to the design of crown ether type complexes based on construction of hydrogen-bonded host supermolecules. The host species, called a cylamer, is composed of small molecules which associate via hydrogen bonding into discrete ring-shaped aggregates. Similar kinds of cavities have been seen before in crystals of trimesic acid[5] and more recently in rigid bicyclic diol crystals,[6] but these structures contain infinite two-dimensional hydrogen-bonded networks rather than the discrete hydrogen-bonded aggregates that characterize cyclamers. While cyclamers could, in principle, exist in solution as analogues of σ-bonded crown ethers, trimesic acid and bicyclic diol hosts could not.

An example of a hydrogen-bonded host-guest species which can exist independently of its crystal structure is the water gas hydrate, one of the first structurally characterized clathrates.[7] The aqueous host in the gas hydrates differs from cyclamers primarily in that it is inorganic and it forms a spherical cavity rather than a ring. Organic hydrogen-bonded complexes are also known, for example, hydroquinone[8] and Dianin's compound,[9] both of which

* Permanent address: Polish Academy of Sciences, Warsaw, Poland.
† University of Minnesota.
‡ Colorado State University.

(1) (a) Lehn, J. M. *Science (Washington, D.C.)* **1985**, *227*, 849. (b) Cram, D. J. *Science (Washington, D.C.)* **1983**, *219*, 1177.
(2) Pedersen, C. J.; Frensdorff, H. K. *Angew. Chem., Int. Ed. Engl.* **1972**, *11*, 16.
(3) Newcomb, M.; Cram, D. J. *J. Am. Chem. Soc.* **1975**, *97*, 1257.
(4) (a) Weber, E.; Josel, H.-P.; Puff, H.; Franken, S. *J. Org. Chem.* **1985**, *50*, 3125. (b) Bradshaw, J. S.; Chamberlin, D. A.; Harrison, P. E.; Wilson, P. E.; Arena, G.; Dalley, N. K.; Lamb, J. D.; Izatt, R. M.; Marin, F. G.; Grant, D. M. *J. Org. Chem.* **1985**, *50*, 3065. (c) Vögtle, F.; Muller, W. M.; Watson, W. H. *Top. Curr. Chem.* **1985**, *125*, 131.
(5) (a) Duchamp, D. J. *Acta Crystallogr., Sect. B* **1969**, *B25*, 5. (b) Herbstein, F. H.; Kapon, M.; Reisner, G. M. *Acta Crystallogr., Sect. B* **1985**, *B41*, 348.
(6) Bishop, R.; Dance, I. G.; Hawkins, S. C. *J. Chem. Soc., Chem. Commun.* **1983**, 889.
(7) (a) Powell, H. M. *J. Chem. Soc.* **1948**, 61. (b) Jeffrey, G. A.; McMullan, R. K. *Prog. Inorg. Chem.* **1967**, *8*, 43. (c) Davidson, D. W. *Clathrate Hydrates*; Franks, F., Ed.; Plenum: New York, 1973; Vol. 2, Chapter 3.

0002-7863/86/1508-5871$01.50/0